Universal Journal of Carbon Research
https://ojs.wiserpub.com/index.php/UJCR/

Research Article

Iridescent Patterns Production from Solid Film Cellulose Nanocrystals Prepared from Coffee Husks

Catherine Nyaruai*, Moses Ollengo, Gerald Muthakia

Chemistry/School of Science, Dedan Kimathi University of Technology, Nyeri, Kenya
E-mail: catenyaruai@gmail.com

Received: 29 April 2024; **Revised:** 12 June 2024; **Accepted:** 13 June 2024

Abstract: The dire need for environmental conservation has spurred the exploration of novel approaches for developing biodegradable and sustainable materials sourced from natural origins, particularly for engineering applications and these include cellulose. Utilizing coffee husks, a waste product from coffee production, offers a sustainable source of cellulose, effectively diverting waste from the environment and turning it into a valuable and profitable resource. The cellulose content within coffee husks were extracted through alkaline treatment, after which, acid hydrolysis was done, yielding cellulose nanocrystals (CNCs) that were utilised to create iridescent films. The process involved treating the coffee husks with sodium hydroxide to obtain cellulose, followed by bleaching with sodium hypochlorite. Acid hydrolysis using gaseous HCl was then employed yielding cellulose nanocrystals. The application of HCl improved the iridescent film quality for secure sheets by preventing the whiskers that are usually seen when sulfuric acid is used. This raises the overall quality and security of the finished product. To avoid contamination, the CNC suspension was carefully transferred into Petri dishes made of polystyrene, and the suspension evaporated at controlled temperature in an oven, resulting in a solid CNC film. To introduce patterns on the film, the Petri dish containing the CNC suspension was placed on a mold engraved with a specific pattern. Heating of the mold imparted different colors onto the film. The outcome of heating the CNC Suspension involved the self-assembly of CNCs into a multitude of colorful and iridescent films possessing unique optical properties. Additionally, these films exhibited water resistance, luminous color variations based on viewing angles, fluorescence, and reflection of left-handed circularly. The value addition of coffee husk waste, which makes it a cleaner environmental product while producing security sheets, is the significance of this work particularly the inclusion of cyclic redundancy, which guarantees improved security features.

***Keywords*:** cellulose nanocrystals; pattern forming object; optical variable devices; iridescent film; circularly polarized light

1. Introduction

Coffee is a crucial agricultural product and one of the leading agricultural commodities globally. An average of 167.26 million bags of coffee were consumed in the year 2020–2021, representing a 1.9% increase compared to the previous year. However, coffee production generates significant waste during processing, with over 50% of the coffee bean being discarded [1]. These waste products, including coffee husks and pulp, are currently not fully utilized profitably and are often inappropriately discarded, leading to environmental concerns due to their organic compound content [2]. Annually, global coffee production generates millions of tons of byproducts, with

Copyright ©2024 Catherine Nyaruai, et al.
DOI: https://doi.org/10.37256/2120244851
This is an open-access article distributed under a CC BY license
(Creative Commons Attribution 4.0 International License)
https://creativecommons.org/licenses/by/4.0/

coffee husks comprising a substantial share. The production volume of coffee husks varies yearly, driven by factors including consumption patterns, harvest yields, and processing methods. Leading coffee-producing nations such as Brazil, Vietnam, Colombia, Indonesia, and Ethiopia play a significant role in coffee husk production owing to their extensive coffee cultivation practices [3].

Coffee husks typically contain varying amounts of cellulose, hemicellulose, lignin, and other organic compounds. Cellulose, a vital polysaccharide forming the structural component of plant cell walls, is particularly noteworthy for its potential industrial applications. Studies have indicated cellulose content in coffee husks ranging from 30% to 50%, positioning them as a promising source of renewable cellulose for various industrial processes [4]. Cellulose, the most abundant natural linear biopolymer, possesses exceptional mechanical properties. With the growing emphasis on environmental conservation, there is a strong research focus on producing biodegradable and green bio-based products from natural sources for various engineering applications [5, 6]. Various effective methods have emerged for utilizing coffee husks. These include their use as a feedstock for biofuel production through pyrolysis or fermentation processes. Once treated to eliminate caffeine and tannins, they become valuable feed supplements for livestock. Composting coffee husks generates nutrient-rich organic fertilizer, enhancing soil fertility and plant growth. They can also be integrated into biocomposite materials for diverse industrial applications such as construction and packaging. Some studies explore their potential in adsorbing pollutants from wastewater, aiding in environmental cleanup. Moreover, extracts from coffee husks contain bioactive compounds with antioxidant and antimicrobial properties, presenting opportunities for incorporation into functional foods and beverages [7]. Utilizing agro-wastes, including coffee husks, offers an opportunity to add value to waste products and develop renewable and profitable materials [8]. The cellulose in coffee husks was extracted through a process involving treatment with sodium hydroxide, bleaching with hydrogen peroxide, and subsequent treating with hydrochloric acid, resulting in cellulose nanocrystals (CNC).

Nanotechnology, involving the manipulation of matter on a near-atomic scale and offering the potential to create new structures, materials, and devices, finds applications in various fields, including pulp and paper.[9, 10]. Nanotechnology has provided opportunities for enhancing the properties of packaging materials, such as increased strength, resistance to water and fire, and antimicrobial properties, thereby benefiting the pulp and paper industry [11].

The conversion of cellulose into cellulose nanocrystals (CNC) has shown promise, and advanced technologies, such as chemical and enzymatic pre-treatment, can effectively minimize the associated energy-intensive and costly challenges [12]. Acid hydrolysis is the preferred method for converting cellulose into nanocrystals. CNC finds applications in materials engineering, biodegradable packaging, aerospace and automotive industries, drug delivery, wound healing patches, electronics, and coatings [13]. In the realm of paper, CNC enhances surface gloss, mechanical properties, and printability of coated papers. The unique properties of CNC, including its ability to form an iridescent film with desirable optical characteristics due to the presence of hydroxyl groups, make it suitable for applications such as generating optical security seals.

Security features are categorized into three levels: overt, covert, and forensic. Cellulose nanocrystals (CNC) self-assemble into colorful and iridescent films with unique optical properties, including color-shifting and left-handed circular polarization, providing covert security. The cost-effectiveness and simplicity of producing CNC-based iridescent films make them suitable for various applications, such as medicinal seals and money security, while their integration can make counterfeiting nearly impossible [14].

The reference underscores the environmental significance of coffee waste pollution, particularly in Central America, emphasizing its detrimental effects on ecosystems and water sources due to improper disposal practices. It also highlights the hazardous compounds in coffee bean husks. The referenced work seeks to address this urgent issue [15, 16].

Coffee husks were utilized in this study as a promising solution to address environmental concerns. The extracted cellulose from coffee husks can be further processed into cellulose nanocrystals, which have the potential to create advanced iridescent optical security features, thereby enhancing information security and authentication methods. Researchers from diverse fields are increasingly drawn to sustainable biomaterials as alternatives to petroleum-based ones due to their renewable nature, biodegradability, and reduced reliance on harmful additives, addressing sustainability concerns [17].

Recent cyber-attacks have driven the development of advanced optical security features, including two-piece meta-material systems and cellulose nanocrystals, to enhance forgery protection and information encryption, offering increased security for high-value items like banknotes [18]. Cellulose nanocrystals can be utilized to produce iridescent films that serve as optical security features.

2. Related Work

Research on coffee husks has examined their composition as well as the degree of environmental contamination they cause. To identify the chemical components and possible uses of coffee husks, researchers have carefully examined their complex composition. Furthermore, the purpose of these studies has been to clarify the ecological effects of coffee husk disposal by explaining the potential effects of their decomposition or incineration on the quality of the air, soil, and water. Scientists examine the quantitative and qualitative characteristics of coffee husks in order to develop sustainable management strategies that will lessen their negative environmental impact [1, 16, 19–25].

An extensive body of research has been conducted on the structure and connections of cellulose, using a variety of extraction techniques to separate this essential biopolymer from its precursor materials. Scholars have laboriously scrutinised the complex structure of cellulose molecules, unravelling the complexities of its polymer chains and intermolecular bonding. In addition, a wide range of extraction methods have been used, each specifically designed to maximise the yield and purity of cellulose, from conventional chemical treatments to state-of-the-art enzymatic procedures. Researchers work to fully realise the potential of cellulose in a variety of applications, from cutting-edge biomedical scaffolds to sustainable packaging materials, by improving extraction procedures. A new era of sustainable materials is being ushered in by the scientific community's multidisciplinary efforts to maximise cellulose's versatility while reducing its environmental impact [26–30].

This study explores the complex field of cellulose extraction by employing Bronsted acids in conjunction with an alkaline treatment and acid hydrolysis approach. The objective of the research was to obtain the best possible cellulose yield and purity from the source material by utilising these flexible techniques. The process of alkaline treatment breaks the bonds that bind cellulose to other substances, which makes it easier to separate the cellulose fibres later on. On the other hand, cellulose can be broken down into its component glucose units by acid hydrolysis, which offers important information about the structural characteristics of cellulose. Bronsted acid additions also give the extraction process a catalytic component, which improves selectivity and efficiency. This work illuminates the cooperative interaction between various extraction techniques via rigorous testing and analysis, opening the way for advancements in cellulose research and applications [31, 32].

The way in which the rod-like shapes are arranged strategically is crucial to understanding how the iridescent film is produced and how it evokes the enthralling iridescence that is seen. In order to achieve the desired iridescent effect, researchers carefully engineered the arrangement of these rod-like structures, utilising their special optical properties. The goal of the project was to identify the fundamental mechanisms guiding the formation of iridescence by carefully manipulating variables like the size, orientation, and spacing of these structures. This work adds to the developing field of photonic materials by clarifying the relationship between structure and optical behaviour, with potential uses ranging from biomedical diagnostics to advanced displays [33–37].

This ground-breaking study demonstrates the transforming potential of coffee husk waste by demonstrating its ability to produce iridescent paper, which adds a substantial value to what was previously thought to be just waste material. Through creative reuse of coffee husks, researchers reduce pollution in the environment and open up new possibilities for the development of sustainable materials. The resulting iridescent paper reflects a paradigm shift towards the ideals of the circular economy, while also captivating with its aesthetic appeal. This creative method not only gives waste streams a real value addition, but it also promotes a resource utilisation strategy that is both economically and environmentally sound. The study highlights the value of innovative thinking and interdisciplinary cooperation in tackling urgent environmental issues and expanding the horizons of material science through such ground-breaking initiatives.

3. Material and Methods

High-quality reagents and chemicals were sourced from Kobian Kenya Limited, an authorized distributor of Sigma Aldrich in Kenya. Distilled water was employed for the formulation of reagents and for dilution purposes. The coffee husks were procured from Dedan Kimathi University's agricultural grounds.

3.1 *Extraction and purification of Cellulose from coffee Husks*

The extraction and purification of cellulose from coffee husks were conducted following a series of well-defined steps. These processes have been described in a previous study [31].

3.1.1 *Alkali Treatment of Cellulose*

The coffee husks underwent air drying and sieving to attain an average particle size ranging from 2 to 3 mm. Subsequently, 4% by weight of finely ground coffee husks was added, establishing a sodium hydroxide-to-water ratio of 1:20. The mixture underwent reflux for a duration of 3 hours with continuous stirring. The resulting solid was filtered and subjected to multiple rinses with distilled water to ensure the complete removal of the alkali. This entire procedure was iterated three times to ensure its comprehensive effectiveness.

3.1.2 *Bleaching Treatment*

During the bleaching procedure, equivalent amounts of sodium chlorite (1.7% by weight), acetate buffer solution, and water were mixed with the solid previously treated with alkali, maintaining a mass ratio of 1:20. The blend was subjected to reflux conditions for 4 hours, and this series of steps was iterated approximately three times until the samples attained full whiteness. Following that, the samples were filtered and subjected to several rinses with distilled water to remove any remnants of the bleaching solution.

3.2 *Extraction and Purification of Cellulose nanocrystals*

3.2.1 *Acid Hydrolysis*

The synthesis of cellulose nanocrystals involved subjecting the obtained bleached sample to acid hydrolysis, following the procedures specified in references [31, 38]. The sample was treated with a solution containing 7.5% of the sample's weight and 36% hydrochloric acid (wt/wt) at a temperature of 50 ºC for 40 minutes, with continuous agitation. Following this, the hydrolysed cellulose sample underwent multiple washes with distilled water using centrifugation at 14,000 rpm for 30 minutes to concentrate the cellulose material and remove excess acid. This washing process continued until a stable pH was reached. The subsequent step involved neutralizing the suspension by introducing a 10% ion resin for a 24-hour period. Afterward, the resin was separated from the suspension via vacuum filtration using a filter, and the resulting CNC suspension filtrate underwent 30 minutes of sonication in an ice bath. Finally, the suspension was refrigerated for further analysis.

3.3 *Generation of Iridescent Patterns on Solid Film of Cellulose Nanocrystals*

Petri dishes made of polystyrene were filled with an aqueous suspension containing cellulose nanocrystals at varied concentrations (10 and 50 grams per liter) that had been quantified. The suspension was then allowed to evaporate in either room temperature or in an oven that was specifically set to 65°C. Solid CNC films weighing between 60 and 70 milligrams on average and having an average thickness of 75 micrometers per film were produced by this process.

In order to create a pattern, the Petri dish with the CNC suspension was placed on top of a metal item with a specific shape that was called the pattern-forming object (PFO). To produce a variety of colors on the film, heating or cooling procedures were applied to the PFO. Ultimately, a thorough examination of the resulting movie was done.

3.4 *Instrumentation*

Using a Fourier Transform Infrared spectrophotometer (JASCO FT/IR-4700) before and after each modification process, attached functional groups were verified and identified. The results included the FTIR results. Scanning Electron Microscopy (SEM) was utilized to analyze the microstructure of the material after different treatments: untreated, alkali-treated, and bleached samples. The samples were stored in desiccators containing P_2O_5 for two weeks at 25 °C before conducting SEM observations. The SEM analysis was performed thrice, and the samples were gold-coated and observed using an accelerating voltage of 15kV. UV/Vis spectrophotometers cover a broad range of wavelengths, usually from about 200nm to 800 nm and XRD analysis involves placing a cellulose sample in the XRD instrument. The X-rays are directed at the sample, and the resulting diffraction pattern (XRD pattern) is recorded. The XRD pattern consists of diffraction peaks at specific angles, which correspond to the spacing between planes of atoms in the crystal lattice.

4. Results and Discussion

4.1 *Extraction and Purification of Cellulose from Coffee Husks*

4.1.1 *Alkali Treatment of Cellulose*

On treatment with the alkali the cellulose changed colour, this is an indicator that hemicellulose was removed. The colour change is illustrated in fig1[39].

Cellulose exhibits a strong, crystalline structure resistant to hydrolysis, whereas hemicellulose, with its lower molecular weight and amorphous structure, readily undergoes hydrolysis and biodegradation through the action of specific enzymes produced by bacteria and fungi [39].

Upon introducing sodium hypochlorite, the cellulose underwent a noticeable transformation from a dark black-brown color to a pristine white shade. This shift serves as a clear indication that the bleaching process occurred, as depicted in figures 2 and 3. The objective of this bleaching was to guarantee that the cellulose no longer exhibited any light-absorbing or light-blocking properties during subsequent analysis and the fabrication of the iridescent film. The mass of the Cellulose obtained was 127 grams.

Figure 1. Coffee husks after alkaline treatment with NaOH. The image depicts coffee husks following treatment with NaOH, resulting in a notable transformation in color to dark brown. This change is attributed to the process of de-lignification and the removal of hemicellulose, which are key steps in the alkaline treatment procedure. The dark brown hue observed in the treated coffee husks signifies the successful alteration of their chemical composition, indicative of potential modifications in their structural properties.

Figure 2. Cellulose initial bleaching. The figure illustrates the cellulose material at the beginning of the bleaching process. Prior to treatment with sodium hypochlorite, the cellulose exhibits a dark black-brown coloration. This initial state serves as a baseline for comparison to subsequent stages of the bleaching process

Figure 3. Cellulose final bleaching. The figure displays the cellulose material after completion of the bleaching process. Following treatment with sodium hypochlorite, the cellulose undergoes a dramatic transformation, transitioning to a pristine white shade. This distinct color change signifies the successful completion of the bleaching process, as depicted in both Figures 2 and 3

4.2 *Characterizing Cellulose Nanocrystals*

4.2.1 *Acid Hydrolysis*

In the realm of scientific practice, precise acid hydrolysis techniques are harnessed to isolate cellulose nanocrystals (CNCs) from their original cellulose origins. This controlled hydrolysis process entails the introduction of acidic sulfate ester groups to the surfaces of CNCs by means of sulfuric acid. This chemical modification imparts a negative charge to the surface of the nanocrystals.[34, 40]. Above a critical concentration,

CNCs possess a rod-like shape and negative surface charge, leading to the formation of electrostatically stable colloidal suspensions that undergo phase separation into an upper random phase and a lower ordered phase, the ordered phase corresponds to a chiral nematic liquid crystal, wherein the CNCs are arranged in pseudoplanes [34].

Cellulose nanocrystals are prepared via acid hydrolysis, a process that breaks down the β-1,4-glycosidic bonds of cellulose, a biopolymer composed of glucose units, resulting in the production of glucose molecules or oligosaccharides [41]. Hydrolysis of cellulose polymers occurs when the β-1,4-glycosidic bonds are cleaved by acids, leading to the formation of glucose or oligosaccharides. There are two main types of cellulose hydrolysis: enzymatic hydrolysis and chemical hydrolysis using dilute or concentrated acids. The characteristics of the cellulose material, temperature, reactant concentrations, and reaction time significantly influence both types of hydrolysis. These factors directly impact the kinetics, energy transfers, and mass transfer during the hydrolysis process.

Enzymatic hydrolysis of cellulose begins with the reaction between an acidic proton and oxygen, forming a conjugated corresponding acid and bonding two glucose units. The cleavage of the C-O bond occurs, followed by the formation of a cyclic carbocation. Rapid addition of water leads to the formation of a sugar molecule and the release of a proton [42]. In the polysaccharide chain, the formation of the intermediate carbocation is faster at the chain end compared to the middle region.

Acid treatment, specifically acid hydrolysis, is the primary method for producing cellulose nanocrystals (CNCs), which are smaller units obtained from the initial cellulose fibers. Cellulose fibers consist of both amorphous and crystalline regions. Through harsh acid treatment, the amorphous regions, which have lower density compared to the crystalline regions, break down, resulting in the release of individual crystallites. These crystals exhibit negatively charged surfaces, enabling their dispersion in water. In aqueous suspension, CNC particles are randomly oriented at low concentrations, forming an isotropic phase. However, as the concentration reaches a critical value, a chiral nematic ordering emerges, transforming the CNC suspensions into an anisotropic chiral nematic liquid crystalline phase [43]. CNC surfaces possess abundant hydroxyl groups, providing sites for various chemical reactions.

During acid treatment, the amorphous regions of cellulose are removed, resulting in the purification of cellulose nanocrystals (CNCs). The hydrolysis process involves the penetration of hydronium ions into the more accessible amorphous regions of cellulose, causing the cleavage of glycosidic bonds and the subsequent release of individual crystallites [44]. These crystallites align parallel to each other, leading to an increase in the overall crystallinity of the cellulose. The chemical structure of cellulose contributes to the high crystallinity observed in CNCs, as each monomer contains three hydroxyl groups that can participate in inter- and intra-molecular hydrogen bonding, resulting in a highly compact system [45]. In the case of hydrochloric acid, it dissociates into H^+ and Cl^- ions.

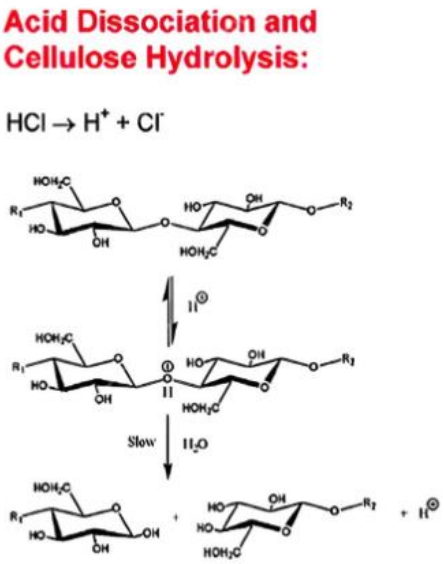

Figure 4. Acid hydrolysis equation. The process of acid hydrolysis acting on cellulose molecules is shown in this image. The amorphous portions of cellulose are broken down more quickly by acid hydrolysis, leaving intact crystalline structures in their place. The reaction that is shown here clarifies the process by which an acid treatment breaks specific bonds in cellulose, causing less ordered areas to degrade while the crystalline cellulose structure is preserved

The reaction is shown in the figure 4. This reaction enables the breakdown of the amorphous parts leaving behind intact crystals that are in suspension just as in figure 5.

To calculate the yield of CNC obtained the formular below was used.

Yield (%) = Final mass of CNCs obtained/Initial mass of cellulose material×100%

Yield (%) = 68.23/125.98*100=54.16%

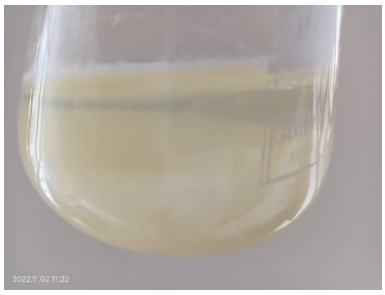

Figure 5. Iridescent Film Formation Using CNC Crystals. This diagram illustrates the generation of an iridescent film utilizing CNC (Cellulose Nanocrystal) crystals. CNC crystals, renowned for their light-bending properties, play a pivotal role in creating the captivating array of color shades observed on the film. The interaction of light with these CNC crystals results in diffraction and interference phenomena, giving rise to the iridescent effect characteristic of the film. This depiction elucidates how CNC crystals contribute to the optical properties of the film, showcasing their potential in innovative material applications

This crystals are used to generate the iridescent film, due to their ability to bend light thus forming the different color shades on the film.

4.3 *Generation of iridescent patterns on solid film of cellulose nanocrystals*

This study successfully showed that iridescent patterns on cellulose nanocrystal (CNC) films can be obtained through a controlled process known as evaporation-induced self-assembly (EISA). In the research, meticulous implementation of EISA facilitated the achievement of mesmerizing and distinct iridescence on solid film CNCs. The CNC suspension exhibited unique anisotropic liquid crystalline behavior, forming left-handed chiral nematic helical structures during this process. These structures involve a periodic rotation in the orientation of the CNC layers, resulting in iridescent colors when the helical pitch 'p' falls within the visible spectrum range. This phenomenon was observed and confirmed through various experimental methods, including polarized optical microscopy.

Furthermore, the specific properties of the CNC suspension and the conditions during film formation allowed manipulation of the chiral nematic pitch and, consequently, the reflected wavelengths and colors. By adjusting factors such as electrolyte concentration and sonication, we could shift the iridescent colors towards shorter or longer wavelengths. The ability to control the reflected colors demonstrated the precision and predictability of the iridescent film fabrication process [40, 43, 46, 47].

Chiral nematic CNC films exhibit the reflection of left-handed circularly polarized light within a wavelength band determined by the pitch. The reflected wavelength, denoted as nP, where n represents the average refractive index of the film (n = 1.55 for CNC), P signifies the chiral nematic pitch, and h represents the angle of reflection with respect to the film's surface. When the value of nP falls between 400 and 700 nm, the reflected wavelength shortens at oblique viewing angles, resulting in the generation of vibrant colors perceived as iridescence. The chiral nematic peak typically occurs within the range of 250 to 450 nm.

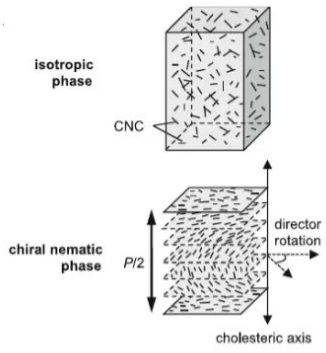

Figure 6. Isotropic and Chiral Nematic Phases of CNC Suspension. This figure illustrates the isotropic and chiral nematic phases observed in the CNC (Cellulose Nanocrystal) suspension. Of particular interest in this research is the chiral nematic phase, characterized by its unique arrangement that enables the reflection of specific wavelengths of light, resulting in the creation of diverse surface color films. The depiction highlights the significance of understanding the structural organization of the chiral nematic phase in leveraging its optical properties for applications in creating vibrant and dynamic color films

By adjusting the electrolyte concentration of the CNC suspension prior to film casting [39] or employing high-energy sonication, which we observed and carried out the reflected colors of iridescent CNC films can be shifted towards shorter wavelengths. In contrast to sulfuric acid, the use of hydrochloric acid reduces interparticle electrostatic repulsion and results in a predictable reduction in pitch. According to Di Giorgio [48], controlled sonication of CNC suspensions can increase the chiral nematic pitch and shift the peak reflection wavelength of resulting films towards longer wavelengths. Typically, the pitch in dried CNC films is comparable to the wavelength of visible light, giving rise to vibrant colors and iridescence that vary with the viewing angle. However, the absence of color and iridescence does not imply the absence of chirality in the films; it simply suggests that the pitch is either red-shifted or blue-shifted beyond the visual range. In certain cases, visibly clear films can be achieved, possibly due to electrostatic effects. By introducing additives, the reflection band in solid chiral nematic CNC films can be selectively shifted towards longer (red-shift) or shorter (blue-shift) wavelengths. This technique alters the heat transfer kinetics in different regions of the evaporating CNC suspension by utilizing pattern-forming objects (PFOs) during film casting. During the film casting process, a predetermined quantity of aqueous CNC solution was applied onto polystyrene Petri dishes. The mixture was subsequently allowed to evaporate under controlled conditions in an oven, typically within the temperature range of 30–50 °C. This process yielded solid CNC films with thicknesses ranging from 60 to 83 µm and an average weight of 65–75 g/m^2. To generate unique patterns, the Petri dish containing the CNC suspension was placed on top of a metal pattern-forming object (PFO), which was either heated accordingly.

Figure 7. CNC suspension in petri dish, in an oven. It illustrates the process of forming a CNC film. Initially, the CNC suspension is placed on a petri dish inside an oven. As the temperature is raised, the CNC suspension evaporates, resulting in the formation of a film. A PFO is positioned below the petri dish during this process

An iridescent solid film with a recognizable pattern in the shape of the PFO is created when CNC suspensions are evaporated with a portion of the container in contact with a pattern-forming object (PFO) at a temperature higher than the surrounding material. The pattern reflects longer wavelengths than the surrounding film areas and has nearly identical dimensions to the PFO, which suggests that the self-assembled chiral nematic structure has a larger pitch. Pattern formation is done by local heating by heating the suspension, in the petri dish and PFO assembly in an oven placed below the petri dish. In relation to the surrounding suspension, a heated or cooled PFO will heat or cool the suspension above it. The vessel containing the CNC suspension is spaced from the heat source when casting CNC films above a PFO in an oven, allowing air to serve as a heat transfer medium to the suspension's components that are not in contact with the PFO.

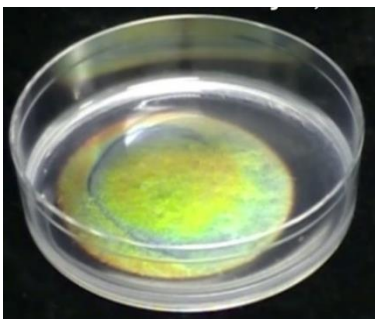

Figure 8. Iridescent film produced. *It shows the iridescent film produced. The film exhibits a distinct color pattern, featuring an outer circular blue pattern, transitioning to a greenish hue, and then to an innermost yellowish area. This sequence represents the characteristic pattern formed*

The temperature of the evaporating suspension controlled by the speed of heat transfer. At a given oven temperature, a good thermal conductor, such as metal, will transfer heat to the suspension more quickly than the surrounding air, producing a zone of higher temperature in the suspension above the metal object. The CNC suspension is visible in the side view sitting atop a thermal conductor PFO half-circle on a metal shelf inside an oven.

The analysis conducted on this iridescent film made from cellulose nanocrystal (CNC) suspension revealed fascinating optical properties. The film exhibited iridescence, displaying a range of colors depending on the viewing angle. The iridescence was a result of the film's chiral nematic structure, where CNCs self-assembled into layers with a characteristic pitch. The wavelength of light reflected by the film governed by this pitch, which produced the colors seen. Within a particular wavelength range, the film selectively repelled left-handed circularly polarized light while transmitted the opposite hand of circular polarization. The optical properties of the chiral nematic film matched that of cholesteric liquid crystals. Understanding the special qualities of CNC-based iridescent films and their possible uses in optics and display technologies made possible by the analysis.

4.4 *FTIR Analysis*

In this work, the coffee husk surface was treated with NaOH alkali to eliminate hemicellulose, lignin, and other undesirable components. The effects of NaOH alkali treatment on the chemical makeup of coffee husks were examined using FTIR analysis [15]. The infrared spectrum showed several distinctive peaks: a broad band from 3400 to 2850 cm^{-1} attributed to C-H bonds commonly found in alkenes; intense peaks at 1730–1732 cm^{-1} and 1450–1650 cm^{-1} indicating C=O groups in ketones and carbonyl groups associated with hemicellulose and lignin compounds, respectively. These broad bands corresponded to hydrogen-bonded OH stretching from cellulose, hemicellulose, and lignin.

For treated coffee husks, the FTIR spectrum showed an O-H absorption band at about 3329.50 cm^{-1}, and for untreated coffee husks, it was 3324.68 cm^{-1}. Untreated coffee husks showed a C-H stretching peak at 2914.88 cm^{-1}, while 10% NaOH-treated coffee husks exhibited a stretching peak at 2908.13 cm^{-1}. Peaks at 1636.30 cm^{-1} and 1636.02 cm^{-1} in untreated and alkali-treated coffee husks, respectively, corresponded to C=O stretching vibrations of acetyl groups in hemicellulose compounds. The intensity of these peaks was not observed in the treated coffee husks due to the NaOH treatment, indicating a reduction in hemicellulose components.

Furthermore, the peaks in the range of 1460–1650 cm^{-1} represented the aromatic structure of lignin in coffee husks. The presence of a peak at 1636.30 cm^{-1} in untreated coffee husk fibers indicated the presence of lignin, which decreased in intensity after NaOH treatment. The region of 1300–1500 cm^{-1} exhibited peaks associated with CH bending of hemicellulose, O-H stretching of cellulose, and C-O stretching of the NaOH group. Peaks at 1372.10 cm^{-1} and 1588.09 cm^{-1} were attributed to acetyl (lignin) C-O stretching and were significantly reduced by the 10% NaOH treatment. Peaks at 1374.03 cm^{-1} and 1372.10 cm^{-1}, representing carbon-hydrogen bending of hemicellulose compounds, were eliminated by NaOH treatment. The peak at 1030.77 cm^{-1} indicated the presence of hydrogen bond groups in cellulose and the occurrence of b-glycoside of the monosaccharide in untreated coffee husks. Treated coffee husks also showed a similar peak at 1026.91 cm^{-1}, indicating that the treatment did not completely remove these groups. The stretching vibrations of -O-H and C-O-C present in lingo-cellulosic materials were represented by peaks in the range of 3330 to 1026 cm^{-1}. Notably, the well-defined peaks at 2914 cm^{-1} and 1588 cm^{-1} corresponded to the stretching and bending vibrations of C-H bonds, respectively. The absence of a peak at 1320 cm^{-1} was attributed to the decrease in lignin and hemicellulose content in the treated coffee husks [15].

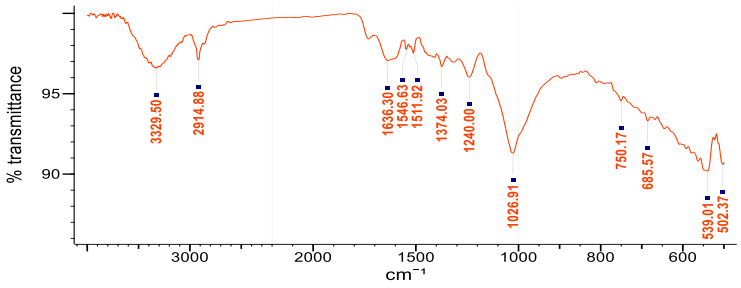

Figure 9. FTIR of Coffee husks. The spectrum displays characteristic absorption bands, indicating the presence of various functional groups and compounds typical of coffee husk composition. These include peaks corresponding to cellulose, hemicellulose, lignin, and other organic constituents

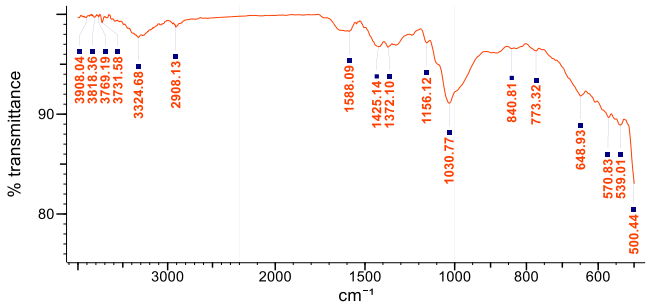

Figure 10. FTIR of cellulose. The spectrum features characteristic absorption bands, including peaks associated with O-H stretching, C-H stretching, and C-O-C stretching vibrations. These bands provide insights into the molecular structure and functional groups present in the cellulose

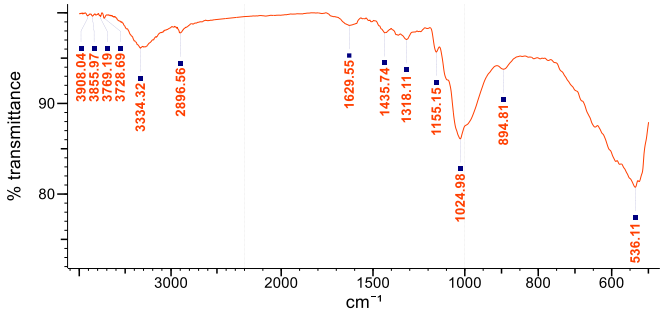

Figure 11. FTIR of Cellulose NanoCrystals. The spectrum showcases distinct absorption bands indicative of key functional groups, such as O-H stretching, C-H stretching, and C-O-C stretching vibrations. These peaks reflect the molecular structure and the nanoscale characteristics of the cellulose nanocrystals

FTIR analysis is a valuable technique for characterizing cellulose by identifying its functional groups, including hydroxyl, carbonyl, and carboxyl groups. Specific infrared absorption bands provide information about these groups: the hydroxyl group stretching vibrations appear around 3400 cm^{-1}, carbonyl group vibrations around 1730 cm^{-1}, and carboxyl group vibrations around 1420 cm^{-1}. Furthermore, at about 2920 cm^{-1} and 2850 $cm^{-1,}$ respectively, stretching vibrations of the CH_2 and CH_3 groups are observed. FTIR analysis makes it easier to determine the crystalline and amorphous regions within the cellulose structure as well as the chemical composition of cellulose, including the presence of functional groups.

4.5 *UV-VIS analysis*

According to my findings, the cellulose nanocrystal (CNC) iridescent film's optical characteristics were greatly enhanced by UV-Vis analysis. Absorption characteristics were found throughout the UV and Vis regions, with particular absorption peaks corresponding to electronic transitions in the film, according to the analysis. The film's iridescence was strongly correlated with absorption maxima that were seen between 480 and 540 nm. Certain bands were associated with iridescence by comparing absorption characteristics with observed colours and spectra. Additionally, the film's energy bandgap was estimated with the aid of UV-Vis analysis, which is crucial for comprehending its optical and electrical characteristics. These results provide useful information for further research and are critical for optimising the film's applications in domains where precise control over light-matter interactions is crucial, such as photonics and optoelectronics [46, 49, 50].

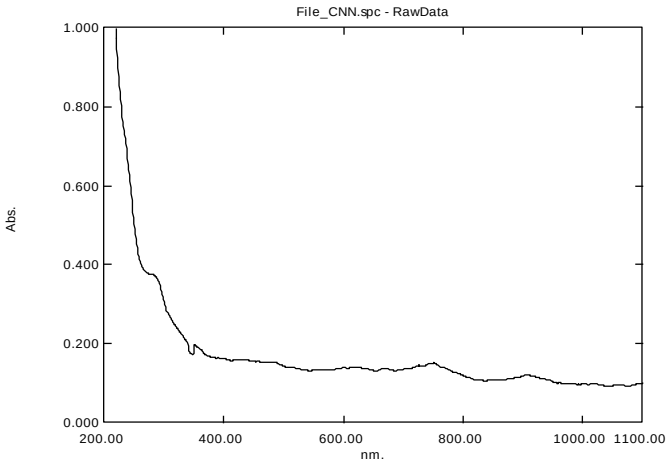

Figure 12. UV-VIS of CNC. The spectrum highlights the absorbance properties of CNCs, demonstrating characteristic peaks that correspond to their optical behavior and electronic transitions. This data provides insights into the light-absorbing features and potential applications of cellulose nanocrystals in various fields

4.6 *X-ray analysis*

In my findings, the structural properties of cellulose and cellulose nanocrystals (CNCs) were examined using X-ray analysis. Techniques for X-ray diffraction (XRD) and scattering revealed information about the orientation, structure, and crystallinity of the crystal. Distinct diffraction peaks, particularly the cellulose Iβ peak at around 2θ = 22°, revealed the cellulose crystalline structure, with additional peaks indicating other lattice planes and providing details on crystallinity and structure. The crystallinity index (CI) was calculated from XRD data and found to be 21.92º, higher values indicating greater crystallinity. An amorphous hump in the XRD pattern represented amorphous regions, reflecting amorphous content and disorder [51, 52], XRD analysis also estimated crystallite size, identified the specific cellulose type present, and used deconvolution procedures to measure crystallinity. Gaussian peak profiles were commonly used for deconvolution, allowing flexible adjustments to crystalline peak properties. XRD patterns also revealed cellulose molecule orientation, evident through peak elongation or splitting, indicating preferential alignment along a particular direction [53, 54] These X-ray analysis results significantly contributed to understanding cellulose's crystalline nature, degree of order, and crystal structure, laying the groundwork for potential applications across various industries. Comparing these findings with those of other researchers may help validate and enhance our understanding of cellulose and CNCs [55, 56].

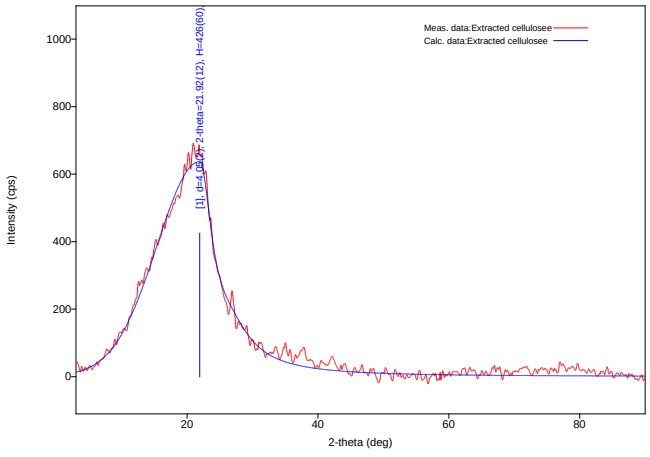

Figure 13. Xray of CNC. The diffraction peaks observed in the pattern correspond to the crystalline structure of the CNCs, revealing information about their crystallinity and lattice arrangement. This analysis is essential for understanding the structural properties of the cellulose nanocrystals

Peak List

No.	2-theta(deg)	d(ang.)	Height(cps)	FWHM(deg)	Int. I(cps deg)	Int. W(deg)	Asym. factor
1	21.92(12)	4.05(2)	426(60)	10.48(17)	5779(101)	14(2)	2.8(2)

Furthermore, XRD patterns provided information about the orientation of cellulose molecules in the material. The elongation or splitting of diffraction peaks indicated preferential orientation, suggesting the alignment of cellulose chains along a particular direction [57]. These results from X-ray analysis on cellulose contributed to a comprehensive understanding of its crystalline nature, degree of order, and crystal structure. They serve as a basis for further studies on cellulose materials and their potential applications in various industries.

4.7 *SEM Analysis*

SEM (Scanning Electron Microscopy) was employed to investigate the shape and size of coffee husks, cellulose and CNC. The coffee husks were grinded then analyzed. The average particle size varies depending on the grinding process, but it typically fell in the micro-meter range of 2.83mm, with some larger and smaller particles present. The distribution was not perfectly uniform [58]. The surface of ground coffee husks appeared rough and irregular under SEM analysis. This roughness was often due to the grinding process, which created fractures and uneven surfaces. Coffee husks contained fibrous components, and SEM analysis showed the structure and arrangement of these fibres. The fibres were at times broken or damaged during the grinding process, resulting in a less organized appearance. The figure 14 shows the coffee husks under SEM analysis.

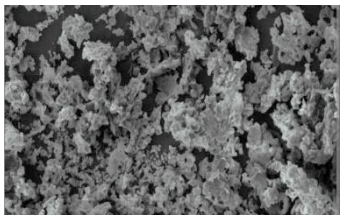

Figure 14. SEM of Coffee husks. The image reveal the surface morphology and microstructural features of the coffee husks, highlighting their fibrous texture, porosity, and the presence of cell wall structures

The coffee husks underwent alkaline treatment to remove the hemi-cellulose and lignin. The figure 15 shows the cellulose attained.

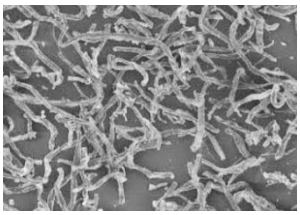

Figure 15. SEM of cellulose. Shows the microstructure of cellulose, revealing its fibrous morphology, hierarchical organization, and surface characteristics. These visualizations offer valuable information about the structural properties and potential applications of cellulose-based materials

Acid hydrolysis method was used to remove the amorphous regions from cellulose fibrils, leading to the formation of CNC bundles, each consisting of individual fibrils. The CNC exhibited a consistent needle-like morphology, measuring 250 nanometers in length and 12 nanometres in diameter, which closely resembled previous findings [59] as shown in the figure 16. As depicted the needle-like cellulose nanocrystal was also evident. The diameter and length distributions of the CNC, presented in displayed a range of 100 to 400 nanometres in length and 4 to 12 nanometres in diameter for the obtained CNC.

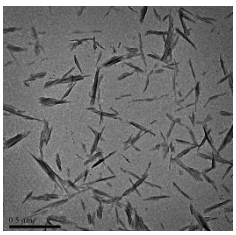

Figure 16. SEM of CNC. The image shows the nanostructured morphology of CNCs, depicting their rod-like shapes, uniform size distribution, and surface characteristics. These visualizations provide insights into the nanoscale features and potential applications of CNCs in various fields

The rod-like CNCs were measured to have an average diameter of 7.97 nanometers, and they exhibited minimal agglomeration. The agglomeration of CNCs may be attributed to the presence of surface ionic charges, which cause the crystallites to stack together during the acid hydrolysis process. Additionally, the aggregation of CNCs could have occurred during the SEM sample preparation when the dispersing medium was removed.

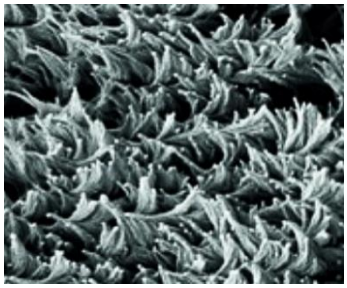

Figure 17. SEM of Iridescent film. Shows the surface morphology and microstructural details of the film, highlighting its layered structure and the arrangement of nanoscale features responsible for the observed iridescence. These visualizations offer insights into the nanostructured architecture and optical properties of the iridescent film

The surface morphology of the iridescent film revealed a textured and patterned surface, which was related to the arrangement of CNCs and the film's iridescence. The distribution of CNCs within the film was observed, and it was noted that the CNCs were evenly dispersed with few regions of agglomeration. Layering was apparent, indicating a stratified structure, and the layering patterns were visualized and analyzed. The crystalline structure of the CNCs in the film was revealed by crystallinity. The crystalline nature of CNCs was indicated by their distinctive needle-like shape. In order to comprehend how CNCs were aligned within the film, orientation was examined. The iridescence and optical characteristics of the film were affected by this alignment. SEM study of an iridescent film fabricated from CNCs provided a thorough grasp of the microstructure and morphology of the film, illuminating the elements that led to its distinct optical characteristics. This data was useful for basic research as well as real-world applications in materials science, optics, and displays, among other areas.

5. Conclusion and Future Scope

The discussion section of the manuscript should come after the methods and results section and before the conclusion. It should relate directly to the questions posed in the introduction and contextualize the results within the literature covered.

6. Conclusions

To sum up, the main result of this work is the creation of an iridescent film, which is a novel accomplishment with potential uses in the manufacturing of secure paper. This work highlights the significance and relevance of security documents in the modern world, with far-reaching implications for the security document industries and the environment. By creating an iridescent film, this paper has demonstrated a ground-breaking invention that has the potential to completely transform the security document market. This technology makes it possible to create complex and almost impossible-to-counterfeit patterns for important documents like identity cards, passports, and

cash—while also providing a more affordable and environmentally responsible option than traditional printing methods.

Using coffee husk waste as a raw material, this work's dedication to green chemistry is among its most important contributions. By doing this, the environmental impact of waste disposal is lessened and sustainability principles and responsible resource management are upheld. This iridescent film has a wide range of potential uses, including packaging, anti-counterfeiting measures for consumer goods, art and design, and secure document production. These industries stand to gain greatly from its integration in terms of financial savings and environmental advantages.

Moreover, the importance of this study lies in the value addition on the coffee husks waste, rendering it an environmental cleaner, while generating security papers. Notably, the incorporation of cyclic redundancy is of paramount importance, ensuring enhanced security features. Additionally, the utilization of hydrochloric acid (HCl) enhances the quality of the iridescent film for secure papers, as it eliminates the formation of whiskers typically observed when using sulfuric acid, thereby improving the overall quality and security of the final product.

Acknowledgments

The authors would like to thank Dedan Kimathi University of Technology (DeKUT) for funding this study

Source of Funding

This study was funded by Dedan Kimathi University of Technology through the graduate assistant sponsorship programme.

Conflict of interest

There is no conflict of interest for this study.

References

[1] Esquivel, P.; Jiménez, V.M. Functional properties of coffee and coffee by-products. *Food Res. Int.* **2011**, *46*, 488–495, https://doi.org/10.1016/j.foodres.2011.05.028.

[2] Polidoro, A.d.S.; Scapin, E.; Lazzari, E.; Silva, A.N.; dos Santos, A.L.; Caramão, E.B.; Jacques, R.A. Valorization of coffee silverskin industrial waste by pyrolysis: From optimization of bio-oil production to chemical characterization by GC × GC/qMS. *J. Anal. Appl. Pyrolysis* **2018**, *129*, 43–52, https://doi.org/10.1016/j.jaap.2017.12.005.

[3] Murthy, P.S.; Naidu, M.M. Sustainable management of coffee industry by-products and value addition—A review. *Resour. Conserv. Recycl.* **2012**, *66*, 45–58, doi:10.1016/j.resconrec.2012.06.005.

[4] Hidayat, E.; Afriliana, A.; Gusmini, G.; Taizo, M.; Harada, H. Evaluate of Coffee Husk Compost. *Int. J. Food, Agric. Nat. Resour.* **2020**, *1*, 37–43, https://doi.org/10.46676/ij-fanres.v1i1.8.

[5] A. B. Balaji, H. Pakalapati, M. Khalid, R. Walvekar, and H. Siddiqui, "Natural and synthetic biocompatible and biodegradable polymers," in Biodegradable and Biocompatible Polymer Composites, Elsevier, 2018, pp. 3–32. doi: 10.1016/B978-0-08-100970-3.00001-8.

[6] M. Bassas-Galia, S. Follonier, M. Pusnik, and M. Zinn, "Natural polymers," in Bioresorbable Polymers for Biomedical Applications, Elsevier, 2017, pp. 31–64. doi: 10.1016/B978-0-08-100262-9.00002-1.

[7] S. S. Kumar, T. S. Swapna, and A. Sabu, "Coffee Husk: A Potential Agro-Industrial Residue for Bioprocess," in Waste to Wealth, R. R. Singhania, R. A. Agarwal, R. P. Kumar, and R. K. Sukumaran, Eds., in Energy, Environment, and Sustainability. , Singapore: Springer Singapore, 2018, pp. 97–109. doi: 10.1007/978-981-10-7431-8_6.

[8] Mondal, S.; Rana, U.; Malik, S. Reduced Graphene Oxide/Fe_3O_4/Polyaniline Nanostructures as Electrode Materials for an All-Solid-State Hybrid Supercapacitor. *J. Phys. Chem. C* **2017**, *121*, 7573–7583, https://doi.org/10.1021/acs.jpcc.6b10978.

[9] *Sustainable Polymer Composites and Nanocomposites*; Springer Science and Business Media LLC: Dordrecht, GX, Netherlands, 2019; ISBN: .

[10] López-Rubio, A.; Fabra, M.J.; Martínez-Sanz, M. Food Packaging Based on Nanomaterials. *Nanomaterials* **2019**, *9*, 1224, https://doi.org/10.3390/nano9091224.
[11] Samyn, P.; Barhoum, A.; Öhlund, T.; Dufresne, A. Review: nanoparticles and nanostructured materials in papermaking. *J. Mater. Sci.* **2017**, *53*, 146–184, https://doi.org/10.1007/s10853-017-1525-4.
[12] Das, A.K.; Islam, N.; Ashaduzzaman; Nazhad, M.M. Nanocellulose: its applications, consequences and challenges in papermaking. *J. Packag. Technol. Res.* **2020**, *4*, 253–260, https://doi.org/10.1007/s41783-020-00097-7.
[13] Xie, S.; Zhang, X.; Walcott, M.P.; Lin, H. Applications of Cellulose Nanocrystals: A Review. *Eng. Sci.* **2018**, https://doi.org/10.30919/es.1803302.
[14] C. Monnet, "Counterfeiting and inflation," p. 24.
[15] Amena, B.T.; Altenbach, H.; Tibba, G.S.; Hossain, N. Physico-Chemical Characterization of Alkali-Treated Ethiopian Arabica Coffee Husk Fiber for Composite Materials Production. *J. Compos. Sci.* **2022**, *6*, 233, https://doi.org/10.3390/jcs6080233.
[16] B. Tolessa, B. T. Amena, H. Altenbach, G. S. Tibba, and H. G. Lemu, "Analysis of the Negative Impacts of Coffee Husk on the Local Environment," In Review, preprint, Jan. 2022. doi: 10.21203/rs.3.rs-1178642/v1.
[17] Collazo-Bigliardi, S.; Ortega-Toro, R.; Boix, A.C. Isolation and characterisation of microcrystalline cellulose and cellulose nanocrystals from coffee husk and comparative study with rice husk. *Carbohydr. Polym.* **2018**, *191*, 205–215, https://doi.org/10.1016/j.carbpol.2018.03.022.
[18] Bakan, G.; Ayas, S.; Serhatlioglu, M.; Dana, A.; Elbuken, C. Reversible decryption of covert nanometer-thick patterns in modular metamaterials. *Opt. Lett.* **2019**, *44*, 4507–4510, https://doi.org/10.1364/ol.44.004507.
[19] D. C. Preethu, "Maturity Indices as an Index to Evaluate the Quality of Compost of Coffee Waste Blended with Other Organic Wastes," Sustain. Solid Waste Manag., p. 6.
[20] Fernandes, A.; Mello, F.; Filho, S.T.; Carpes, R.; Honório, J.; Marques, M.; Felzenszwalb, I.; Ferraz, E. Impacts of discarded coffee waste on human and environmental health. *Ecotoxicol. Environ. Saf.* **2017**, *141*, 30–36, https://doi.org/10.1016/j.ecoenv.2017.03.011.
[21] Miyashira, C.H.; Tanigushi, D.G.; Gugliotta, A.M.; Santos, D.Y. Influence of caffeine on the survival of leaf-cutting ants *Atta sexdens rubropilosa* and *in vitro* growth of their mutualistic fungus. *Pest Manag. Sci.* **2011**, *68*, 935–940, https://doi.org/10.1002/ps.3254.
[22] Alkhatib, R.; Alkhatib, B.; Al-Quraan, N.; Al-Eitan, L.; Abdo, N.; Muhaidat, R. Impact of exogenous caffeine on morphological, biochemical, and ultrastructural characteristics of Nicotiana tabacum. *Biol. Plant.* **2016**, *60*, 706–714, https://doi.org/10.1007/s10535-016-0600-z.
[23] Sledz, W.; Los, E.; Paczek, A.; Rischka, J.; Motyka, A.; Zoledowska, S.; Piosik, J.; Lojkowska, E. Antibacterial activity of caffeine against plant pathogenic bacteria. *Acta Biochim. Pol.* **2015**, *62*, 605–612, https://doi.org/10.18388/abp.2015_1092.
[24] Janissen, B.; Huynh, T. Chemical composition and value-adding applications of coffee industry by-products: A review. *Resour. Conserv. Recycl.* **2017**, *128*, 110–117, https://doi.org/10.1016/j.resconrec.2017.10.001.
[25] Moore, M.T.; Greenway, S.L.; Farris, J.L.; Guerra, B. Assessing Caffeine as an Emerging Environmental Concern Using Conventional Approaches. *Arch. Environ. Contam. Toxicol.* **2007**, *54*, 31–35, https://doi.org/10.1007/s00244-007-9059-4.
[26] C. Brigham, "Biopolymers," in Green Chemistry, Elsevier, 2018, pp. 753–770. doi: 10.1016/B978-0-12-809270-5.00027-3.
[27] F.-W. Bai, S. Yang, and N. W. Y. Ho, "Fuel Ethanol Production From Lignocellulosic Biomass," in Comprehensive Biotechnology, Elsevier, 2019, pp. 49–65. doi: 10.1016/B978-0-444-64046-8.00150-6.
[28] Ismail, I.; Sa'adiyah, D.; Rahajeng, P.; Suprayitno, A.; Andiana, R. Extraction of cellulose microcrystalline from galam wood for biopolymer. PROCEEDINGS OF THE 3RD INTERNATIONAL CONFERENCE ON MATERIALS AND METALLURGICAL ENGINEERING AND TECHNOLOGY (ICOMMET 2017) : Advancing Innovation in Materials Science, Technology and Applications for Sustainable Future. LOCATION OF CONFERENCE, IndonesiaDATE OF CONFERENCE; p. 020072.
[29] Jahan, M.S.; Saeed, A.; He, Z.; Ni, Y. Jute as raw material for the preparation of microcrystalline cellulose. *Cellulose* **2011**, *18*, 451–459, doi:10.1007/s10570-010-9481-z.
[30] Khenblouche, A.; Bechki, D.; Gouamid, M.; Charradi, K.; Segni, L.; Hadjadj, M.; Boughali, S. Extraction and characterization of cellulose microfibers from Retama raetam stems. *Polim. E Tecnol.* **2019**, *29*, https://doi.org/10.1590/0104-1428.05218.
[31] Johar, N.; Ahmad, I.; Dufresne, A. Extraction, preparation and characterization of cellulose fibres and nanocrystals from rice husk. *Ind. Crop. Prod.* **2012**, *37*, 93–99, https://doi.org/10.1016/j.indcrop.2011.12.016.
[32] Mussatto, S.I.; Machado, E.M.; Carneiro, L.M.; Teixeira, J.A. Sugars metabolism and ethanol production by different yeast strains from coffee industry wastes hydrolysates. *Appl. Energy* **2012**, *92*, 763–768, https://doi.org/10.1016/j.apenergy.2011.08.020.

[33] Elazzouzi-Hafraoui, S.; Putaux, J.-L.; Heux, L. Self-assembling and Chiral Nematic Properties of Organophilic Cellulose Nanocrystals. *J. Phys. Chem. B* **2009**, *113*, 11069–11075, https://doi.org/10.1021/jp900122t.
[34] Revol, J.-F.; Bradford, H.; Giasson, J.; Marchessault, R.; Gray, D. Helicoidal self-ordering of cellulose microfibrils in aqueous suspension. *Int. J. Biol. Macromol.* **1992**, *14*, 170–172, doi:10.1016/s0141-8130(05)80008-x.
[35] N. Dabas and G. Jaiswar, "Fundamentals of processing and characterization of polysaccharide nanocrystal–based materials," in Innovation in Nano-Polysaccharides for Eco-sustainability, Elsevier, 2022, pp. 61–81. doi: 10.1016/B978-0-12-823439-6.00014-3.
[36] Habibi, Y.; Lucia, L.A.; Rojas, O.J. Cellulose nanocrystals: Chemistry, self-assembly, and applications. *Chem. Rev.* **2009**, *110*, 3479–3500, https://doi.org/10.1021/cr900339w.
[37] Beck-Candanedo, S.; Roman, M.; Gray, D.G. Effect of Reaction Conditions on the Properties and Behavior of Wood Cellulose Nanocrystal Suspensions. *Biomacromolecules* **2005**, *6*, 1048–1054, doi:10.1021/bm049300p.
[38] Fabra, M.J.; Lopez-Rubio, A.; Lagaron, J.M. High barrier polyhydroxyalcanoate food packaging film by means of nanostructured electrospun interlayers of zein. *Food Hydrocoll.* **2012**, *32*, 106–114, https://doi.org/10.1016/j.foodhyd.2012.12.007.
[39] Cheng, M.; Qin, Z.; Chen, Y.; Hu, S.; Ren, Z.; Zhu, M. Efficient Extraction of Cellulose Nanocrystals through Hydrochloric Acid Hydrolysis Catalyzed by Inorganic Chlorides under Hydrothermal Conditions. *ACS Sustain. Chem. Eng.* **2017**, *5*, 4656–4664, https://doi.org/10.1021/acssuschemeng.6b03194.
[40] Dong, X.M.; Revol, J.-F.; Gray, D.G. Effect of microcrystallite preparation conditions on the formation of colloid crystals of cellulose. *Cellulose* **1998**, *5*, 19–32, doi:10.1023/a:1009260511939.
[41] Torget, R.W.; Kim, J.S.; Lee, Y.Y. Fundamental Aspects of Dilute Acid Hydrolysis/Fractionation Kinetics of Hardwood Carbohydrates. 1. Cellulose Hydrolysis. *Ind. Eng. Chem. Res.* **2000**, *39*, 2817–2825, https://doi.org/10.1021/ie990915q.
[42] D. Fengel and G. Wegener, Wood: chemistry, ultrastructure, reactions. Berlin ...: de Gruyter, 1989.
[43] Revol, J.-F.; Bradford, H.; Giasson, J.; Marchessault, R.; Gray, D. Helicoidal self-ordering of cellulose microfibrils in aqueous suspension. *Int. J. Biol. Macromol.* **1992**, *14*, 170–172, doi:10.1016/s0141-8130(05)80008-x.
[44] De Souza Lima, M.M.; Borsali, R. Rodlike Cellulose Microcrystals: Structure, Properties, and Applications. *Macromol. Rapid Commun.* **2004**, *25*, 771–787, doi:10.1002/marc.200300268.
[45] Siqueira, G.; Bras, J.; Dufresne, A. Cellulosic Bionanocomposites: A Review of Preparation, Properties and Applications. *Polymers* **2010**, *2*, 728–765, https://doi.org/10.3390/polym2040728.
[46] Beck, S.; Bouchard, J.; Berry, R. Controlling the Reflection Wavelength of Iridescent Solid Films of Nanocrystalline Cellulose. *Biomacromolecules* **2010**, *12*, 167–172, https://doi.org/10.1021/bm1010905.
[47] de Vries, H. Rotatory power and other optical properties of certain liquid crystals. *Acta Crystallogr.* **1951**, *4*, 219–226, https://doi.org/10.1107/s0365110x51000751.
[48] Di Giorgio, L.; Martín, L.; Salgado, P.R.; Mauri, A.N. Synthesis and conservation of cellulose nanocrystals. *Carbohydr. Polym.* **2020**, *238*, 116187, https://doi.org/10.1016/j.carbpol.2020.116187.
[49] Bikova, T.; Treimanis, A. UV-absorbance of oxidized xylan and monocarboxyl cellulose in alkaline solutions. *Carbohydr. Polym.* **2004**, *55*, 315–322, https://doi.org/10.1016/j.carbpol.2003.10.005.
[50] Chen, Q.; Liu, P.; Nan, F.; Zhou, L.; Zhang, J. Tuning the Iridescence of Chiral Nematic Cellulose Nanocrystal Films with a Vacuum-Assisted Self-Assembly Technique. *Biomacromolecules* **2014**, *15*, 4343–4350, https://doi.org/10.1021/bm501355x.
[51] Stipanovic, A.J.; Sarko, A. Packing Analysis of Carbohydrates and Polysaccharides. 6. Molecular and Crystal Structure of Regenerated Cellulose II. *Macromolecules* **1976**, *9*, 851–857, https://doi.org/10.1021/ma60053a027.
[52] Kolpak, F.J.; Blackwell, J. Determination of the Structure of Cellulose II. *Macromolecules* **1976**, *9*, 273–278, https://doi.org/10.1021/ma60050a019.
[53] Teeäär, R.; Serimaa, R.; Paakkarl, T. Crystallinity of cellulose, as determined by CP/MAS NMR and XRD methods. *Polym. Bull.* **1987**, *17*, 231–237, https://doi.org/10.1007/bf00285355.
[54] Hult, E.-L.; Iversen, T.; Sugiyama, J. Characterization of the supermolecular structure of cellulose in wood pulp fibres. *Cellulose* **2003**, *10*, 103–110, https://doi.org/10.1023/a:1024080700873.
[55] Garvey, C.J.; Parker, I.H.; Simon, G.P. On the Interpretation of X-Ray Diffraction Powder Patterns in Terms of the Nanostructure of Cellulose I Fibres. *Macromol. Chem. Phys.* **2005**, *206*, 1568–1575, https://doi.org/10.1002/macp.200500008.
[56] He, J.; Cui, S.; Wang, S. Preparation and crystalline analysis of high-grade bamboo dissolving pulp for cellulose acetate. *J. Appl. Polym. Sci.* **2007**, *107*, 1029–1038, https://doi.org/10.1002/app.27061.
[57] Vydrina, I.; Malkov, A.; Vashukova, K.; Tyshkunova, I.; Mayer, L.; Faleva, A.; Shestakov, S.; Novozhilov, E.; Chukhchin, D. A new method for determination of lignocellulose crystallinity from XRD

data using NMR calibration. *Carbohydr. Polym. Technol. Appl.* **2023**, *5*, https://doi.org/10.1016/j.carpta.2023.100305.
[58] Jaramillo, H.Y.; Vasco-Echeverri, O.; Camperos, J.A.G. Characterization of the Coffee Husk: A Potential Alternative for Sustainable Construction. *Civ. Eng. Arch.* **2023**, *11*, 1902–1908, https://doi.org/10.13189/cea.2023.110418.
[59] Sosiati, H.; Muhamin, M.; Purwanto, P.; Wijayanti, D.A.; Triyana, K. Nanocrystalline Cellulose Studied with a Conventional SEM. International Conference on Physics 2014 (ICP-14). LOCATION OF CONFERENCE, IndonesiaDATE OF CONFERENCE.